Enzyme Models

DOI: 10.1002/anie.201403648

Induced-Fit Mechanism in Class I Terpene Cyclases**

Philipp Baer, Patrick Rabe, Katrin Fischer, Christian A. Citron, Tim A. Klapschinski, Michael Groll, and Jeroen S. Dickschat**

Abstract: *We present crystallographic and functional data of selina-4(15),7(11)-diene synthase (SdS) from Streptomyces pristinaespiralis in its open and closed (ligand-bound) conformation. We could identify an induced-fit mechanism by elucidating a rearrangement of the G1/2 helix-break motif upon substrate binding. This rearrangement highlights a novel effector triad comprising the pyrophosphate sensor Arg178, the linker Asp181, and the effector Gly182-O. This structural motif is strictly conserved in class I terpene cyclases from bacteria, fungi, and plants, including epi-isozizaene synthase (3KB9), aristolochene synthase (4KUX), bornyl diphosphate synthase (1N20), limonene synthase (2ONG), 5-epi-aristolochene synthase (5EAT), and taxa-4(5),11(12)-diene synthase (3P5R). An elaborate structure-based mutagenesis in combination with analysis of the distinct product spectra confirmed the mechanistic models of carbocation formation and stabilization in SdS.*

Terpenes, the largest class of natural products, are formed by terpene cyclases from linear oligoprenyl diphosphate precursors. These sophisticated enzymes convert the oligoprenyl diphosphates via cationic intermediates into structurally complex (poly)cyclic hydrocarbons.[1] Class I terpene cyclases bind their substrate by coordination of the diphosphate to a trinuclear Mg^{2+} cluster which itself is bound to the aspartate-rich DDxxD motif and the NSE triad ND(L/I/V)xSxxxE. This structural arrangement is seen in various enzymes from bacteria,[2] fungi,[3,4] and plants.[5,6] After substrate binding an allyl cation is formed by abstraction of pyrophosphate (PP_i). Subsequently, a first cyclization step takes place by an intramolecular attack of an olefinic double bond on the allyl cation at C1. As we have recently reported, this is accomplished with participation of a key carbonyl oxygen atom, located on the central G1/2 helix-break motif, and of the corresponding helix dipole. Both components are perfectly orientated to stabilize the positive charge at the C1 position.[7] The resulting cation may undergo further cyclization in a similar fashion. The cyclization cascade is terminated by deprotonation or by the addition of H_2O.[8–11] Besides these well-known aspects there exist only limited insights into the formation and regulation of the initial carbocation upon substrate binding.[2,12]

The overall amino acid sequence identity of terpene cyclases is weak, while the enzyme structures share a common α-helical fold.[13,14] Upon metal ion and substrate binding structural changes between the open (apo) and closed (ligand bound) enzyme state can be observed, but the conformational rearrangement of enzymes from plants[5,15] and fungi[3,4] display some distinct differences. Recently, structural data of the bacterial *epi*-isozizaene synthase (EIZS) from *Streptomyces coelicolor* bound to PP_i-$(Mg^{2+})_3$-BTAC (benzyltriethylammonium cation), EIZS bound to four Hg^{2+}, and the ligand-free D99N mutant were determined.[2] In comparison to the PP_i-$(Mg^{2+})_3$-BTAC bound enzyme, the EIZS-$(Hg^{2+})_4$ complex showed an extensive conformational rearrangement of helix G, but it remained unclear whether this displays the natural situation of ligand-free EIZS or is an artificial situation owing to Hg^{2+} binding. This is further questioned by the ligand-free D99N mutant that did not show this rearrangement in helix G. Other structural data of bacterial terpene cyclases were obtained either only in a substrate bound or ligand-free state,[12,16] and did thus not allow for conclusive insights into the substrate binding induced incidents. Herein we report on the structure of the bacterial selinadiene synthase (SdS) from *Streptomyces pristinaespiralis* in the ligand-free open conformation, in complex with $(Mg^{2+})_3$ as well as the non-reactive substrate surrogate 2,3-dihydrofarnesyl diphosphate (DHFPP), and in complex with $(Mg^{2+})_3$-PP_i, giving first insights into the dynamic events of a bacterial terpene cyclase.

For our detailed mechanistic studies the terpene cyclase gene of the actinobacterium *Streptomyces pristinaespiralis* ATCC 25486 (accession number WP 005317515)[17] was cloned and expressed in *Escherichia coli*, followed by purification of the protein in its active form. SdS was incubated with a series of natural (oligo)prenyl diphosphates, including dimethylallyl-PP (DMAPP), geranyl-PP (GPP), farnesyl-PP (FPP), and geranylgeranyl-PP (GGPP), as well as the non-natural substrate analogues (2*Z*,6*E*)-FPP, 2-fluoro-

[*] P. Rabe,[+] C. A. Citron, T. A. Klapschinski, Prof. Dr. J. S. Dickschat
Kekulé-Institut für Organische Chemie und Biochemie
Universität Bonn
Gerhard-Domagk-Strasse 1, 53121 Bonn (Germany)
and
Institut für Organische Chemie
Technische Universität Braunschweig
Hagenring 30, 38106 Braunschweig (Germany)
E-mail: j.dickschat@tu-bs.de
P. Baer,[+] K. Fischer, Prof. Dr. M. Groll
Center for Integrated Protein Science at the Department Chemie
Lehrstuhl für Biochemie
TU München (Germany)
E-mail: michael.groll@tum.de
[+] These authors contributed equally to this work.

[**] We thank the staff of PXI of Paul Scherrer Institute, Swiss Light Source (Villigen, Switzerland) for help with data collection. This work was funded by the Deutsche Forschungsgemeinschaft with a Heisenberg grant (DI1536/4-1) and the grant "Duftstoffe aus Actinomyceten" (DI1536/2-1), and by the Beilstein Institut zur Förderung der Chemischen Wissenschaften with a Ph.D. scholarship (to P.R.).

Supporting information for this article is available on the WWW under http://dx.doi.org/10.1002/anie.201403648.

 © 2014 Wiley-VCH Verlag GmbH & Co. KGaA, Weinheim

FPP (2F-FPP), and DHFPP (for synthesis cf. Figure S1 in the Supporting Information).[18–20] FPP was the only accepted substrate that was converted into selina-4(15),7(11)-diene (**1**) and minor amounts of germacrene B (**2**) (Figure 1, and Supporting Information Table S1). The concomitant formation of the sesquiterpenes **1** and **2** is comprehensible, since **2** is an intermediate along the cyclization cascade from FPP to **1** (Scheme 1). The abstraction of PP_i from FPP yields the allyl cation **A** that is cyclized to **B**, followed by deprotonation to **2**. Its reprotonation-initiated cyclization results in **C** that upon deprotonation gives the main product **1**. The binding of FPP and its surrogates to SdS was qualitatively investigated by Thermofluor-based thermal shift assays (Figure S2).[21]

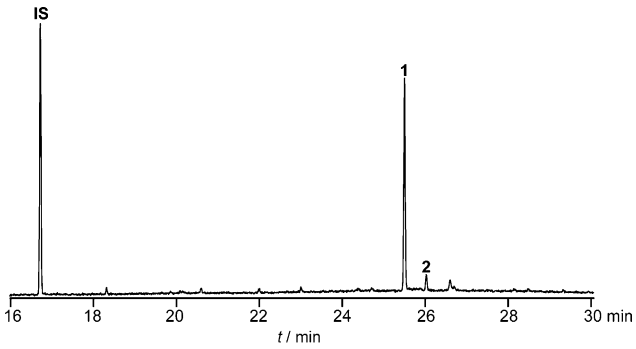

Figure 1. Products of SdS. Total ion chromatogram of an extract from an incubation of FPP with purified SdS. Peak numbers refer to compounds as shown in Scheme 1, IS = internal standard (dodecane).

For detailed insights into the sesquiterpene cyclases' mode of action we determined the crystal structures of SdS in its open (apo, 2.1 Å and $R_{free} = 20.3$) and its closed conformations (bound to DHFPP, 1.9 Å, $R_{free} = 17.7$, and PP_i, 2.1 Å, $R_{free} = 20.3$; Figure 2, Table S2). The monomeric enzyme represents a typical α domain comprising 11 antiparallel helices, which are connected by short linker sequences (Figure S3). The central reaction chamber is formed by helices B, C, G1/2, H, and K, with the DDxxD motif located on helix C and the NSE triad on helix H.[5,12] Upon substrate binding the hydrophobic part of the oligoprenyl diphosphate is orientated into the active site and the C-termini of helices C (^{85}HCEEGELGHR^{94}), H (^{230}HKERRGSG^{237}), and K (^{307}SSVRYTTPDDPANMPS^{322}) get structurally rearranged.[2]

Although four bacterial terpene synthases have already been crystallized[2,7,12,16] and the terpene biochemistry via carbocation intermediates is well documented,[8,22] there is only limited insight into the enzymatic mechanism. So far it has been assumed that carbocation formation in class I terpene cyclases is only metal triggered and takes place upon coordination of the oligoprenyl diphosphate to the $(Mg^{2+})_3$ cluster. Our structural data of SdS now demonstrate the interplay between ligand and enzyme upon substrate binding and active site closure, resulting in a Michaelis complex [SdS:FPP] to initiate product formation. In the course of this reaction sequence, the central G1/2 helix-break motif adopts distinct states between the open (apo) and the closed (substrate bound) conformation, thus following an induced-fit mechanism as revealed by the structural comparison (Figure 3 A). The structural superposition of all bacterial enzymes demonstrates that the overall orientation of helix G1 is strictly conserved, independent of being bound to a ligand or present in the apo state (Figure S4). Notably, the only deviating (artificial) structure is EIZS in complex with 4 Hg^{2+} ions, displaying a significant displacement of the entire G1 helix. Our data highlight a novel effector triad, including a PP_i sensor (Arg178), a linker (Asp181), and an effector (Gly182)

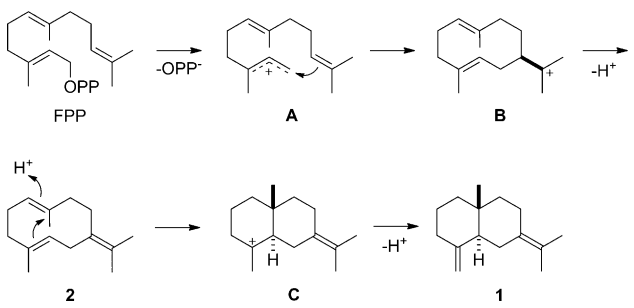

Scheme 1. Cyclization of FPP to **1** by SdS.

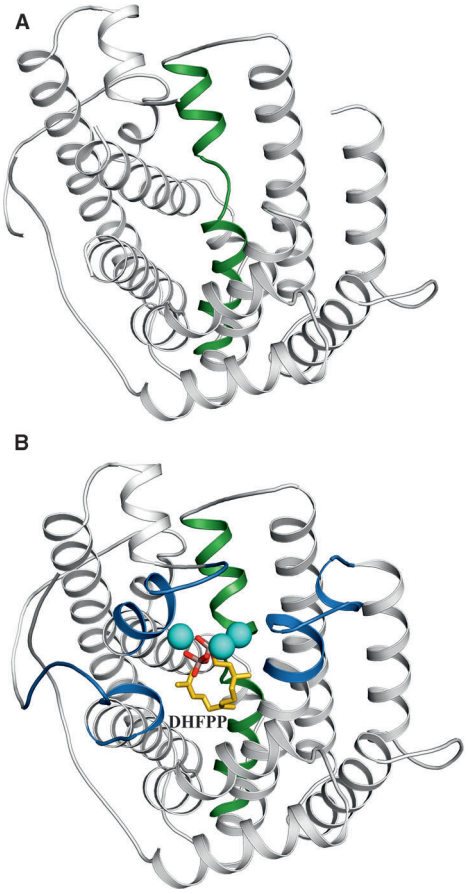

Figure 2. Crystal structures of SdS. A) Ribbon drawing of apo-SdS (open conformation) and B) of SdS in complex with DHFPP (closed conformation). The helix G1/2 is in green, DHFPP yellow, oxygen atoms red, phosphorous dark salmon, and Mg^{2+} cyan. Structural elements which are formed upon DHFPP binding are in blue.

 © 2014 Wiley-VCH Verlag GmbH & Co. KGaA, Weinheim

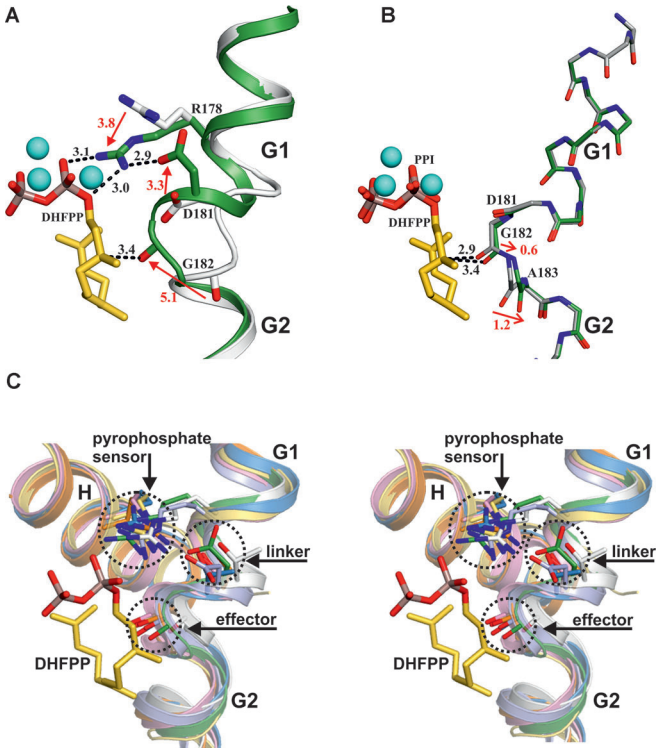

Figure 3. Close up view of helix G1 and the helix-break motif. A) Structural superposition of helix G1/2 in open (apo, light gray) and closed (DHFPP bound, green) conformations; color coding is according to Figure 2. Interactions are depicted as dashed lines; distances are shown in Å. Red arrows highlight the induced fit between the open and the closed conformation. B) Structural overlay of the protein backbone from SdS in complex with PP_i (dark gray) and DHFPP (green). Both complexes resemble the closed conformation. Stereo figures and the F_O–F_C electron-density maps for PP_i and DHFPP are presented in Figures S6 and S7. C) Stereo representation of the structural superposition of the effector triad, comprising the PP_i-sensor, the linker, and the effector residue. SdS:DHFPP (green), EIZS (gray, 3KB9),[2] aristolochene synthase (light blue, 4KUX),[25] bornyl diphosphate synthase (pink, 1N20),[26] limonene synthase (orange, 2ONG),[27] 5-*epi*-aristolochene synthase (blue, 5EAT),[5] and taxadiene synthase (3P5R, yellow).[6]

that is strictly conserved and of general importance for enzyme catalysis in bacterial, fungal, and plant class I terpene cyclases.

Upon substrate binding Arg178 shifts towards the ligand by 3.8 Å, hereby forming two hydrogen bonds (3.1 Å and 3.0 Å) between its guanidino group and PP_i as part of a previously recognized hydrogen-bonding network (Figure 3A).[2–4] Simultaneously, Asp181 is reoriented by 3.3 Å and H-bonded with Arg178 (2.9 Å). This ternary coordination is important for connecting the substrate binding with the conformational change of the G1 helix-break. Therefore, Arg178 is of critical importance for functionality as demonstrated in mutagenesis experiments (see below). This precise modulation proceeds with a conformational change of the whole G1/2 helix-break motif that moves the catalytic key carbonyl oxygen atom of Gly182 (Gly182-O)[5,7] by 5.1 Å inwards into the active site. Its free electron pair directly points towards C3 of DHFPP (3.4 Å) which, in case of binding of the natural substrate FPP, triggers the cleavage and release of PP_i by interacting with the π* molecular orbital of the 2,3 double bond to form the allyl cation **A**. As this functional group is absent in the saturated surrogate, the enzyme in complex with DHFPP is locked in the substrate-bound state, allowing it to mimic the Michaelis complex. Further, the structural data elucidate a plasticity of the helix-break motif, as illustrated by superposition of the helices G1/2 of the SdS:PP_i and the SdS:DHFPP complexes (Figure 3B). This superposition highlights that in the SdS:PP_i complex Gly182-O remains deeply buried in the active site compared to the situation in the SdS:DHFPP structure, indicating that FPP or one of its surrogates provoke steric repulsion in the Michaelis complex state. The effector triad of Arg178, Asp181, and Gly182 is completely structurally conserved in all bacterial, fungal, and plant class I terpene cyclases. In bacteria and fungi the pyrophosphate sensor is located on helix G1, for plants this sensor is found on helix H (Figure 3C, Table S3 and Figure S4).[5,6] Hence, the induced-fit mechanism and substrate ionization by the carbonyl oxygen (Gly182-O in SdS) is—as a rule—relevant for all class I terpene cyclases.

The mechanistic insights from the structural data were confirmed by analysis of 28 site-specific mutants that can be subdivided into three classes according to their proposed roles (Table S1):

1) Hydrophobic and aromatic residues that contour the active site,[12,23,24] stabilize carbocation intermediates,[3,12,22–24] and hence determine the chemical nature of the product
2) Residues involved in substrate binding and/or coordination of the PP_i-$(Mg^{2+})_3$-H_2O cluster
3) Residues with a catalytic function that are involved in the induced fit, the G1/2 helix-break's plasticity, and substrate ionization.

From group (1) several mutations of aromatic residues demonstrated that these play a key role in carbocation stabilization (Phe55, Phe79, Trp304, Tyr311; a detailed discussion of all these mutants is given along with Figure S8–S11). Remarkably, the F55L and F79L mutants showed drastically altered product spectra compared to the wildtype SdS, comprising the linear terpenoids (*E*)-β-farnesene (**5**), (2*Z*,6*E*)-α-farnesene (**6**), and (2*E*,6*E*)-α-farnesene (**7**) in addition to the products **1** and **2** (Figure S8 and S9, depending on the temperature setting of the transfer line of the GC/MS compound **2** may be observed as its thermal Cope rearrangement product **2***). These results are in line with previous reports on EIZS mutants[2] and mark Phe55, with respect to its position towards DHFPP, to be critical for the stabilization of cation **B**, whereas Phe79 is involved in cation–π interaction for stabilization of cation **A**. Furthermore, the Phe79 mutant demonstrates that interaction of cation **C** with aromatic residues is not critical for the formation of **1**. Mutated residues from group (2) are Asp83 (D83N, D83E) and Glu159 (E159Q, E159D). Asp83 is part of the highly conserved DDxxD motif and forms two H-bonds with Arg310 and with a H_2O molecule coordinated to the $(Mg^{2+})_3$ cluster, linking helix K with helix C upon substrate binding. This interdigitating network causes closure of the active site and a defined

 © 2014 Wiley-VCH Verlag GmbH & Co. KGaA, Weinheim

orientation of the PP_i moiety. The replacements D83N and D83E predominantly yield **2**, with a strongly reduced activity in case of D83N, while the conversion into **1** is prevented (Figure S12). Glu159 forms H-bonds to two H_2O molecules coordinated to the $(Mg^{2+})_3$ cluster, which should also be accomplishable by E159Q and E159D. Surprisingly, an almost complete loss of **1** was observed in both mutants (Figure S13). The inactivity of both the Asp83 and Glu159 mutants in the conversion of **2** into **1** is a result of an inaccurate positioning of PP_i that may act as a general acid/base[23] and thus be of critical importance for the protonation of **2** for its conversion into **1**. Next, amino acid residues from group (3) were tested by mutagenesis of Arg178, Asp181, Gly182, Ala183, and Tyr152. The Arg178 PP_i-sensor is H-bonded with its guanidine moiety to the substrate's PP_i and to one oxygen atom of the carboxylate function of Asp181 (Asp181-$O^{\delta1}$). Accordingly, the R178N and R178K mutants are inactive (Figure S14). Asp181-$O^{\delta1}$ also contributes to the helix-break rearrangement upon substrate binding, thereby acting as a linker between the PP_i sensor and the effector Gly182-O. The replacements of D181N and D181S are able to functionally substitute Asp181 in the hydrogen-bonding network, as both mutants produce similar levels of **1** as the wildtype protein (Figure S15). In fact, this linker between Arg178 and Gly182 can be functionally realized by Asp, Thr, Ser, or Asn as found in the respective position among the variety of bacterial sesquiterpene cyclases (Figure S5, position 8). As outlined above, the effector Gly182-O fulfills a key role in catalyzing the abstraction of the PP_i group. The closure of the active site and cation formation were characterized in detail by exchange of Gly182 with two hydrophobic amino acid residues of different size (G182A, G182 V) as well as G182P. Whereas the substitution G182A yields only small amounts of **1** along with a considerable increase of **2**, terpenoid formation is prevented in the G182V mutant (Figure S16). As expected, the G182P substitution fundamentally disturbs the enzyme's conformation at the G1/2 helix break, producing an inactive enzyme. Further structural inspection of wildtype SdS in the open conformation reveals that the side chain of Ala183 causes steric repulsion upon active site closure, followed by a structural rearrangement of Tyr152 by 2.1 Å (Figure S17). If this residue is exchanged by sterically more-demanding residues as in the A183V or A183F mutants, the enzyme is locked in the open conformation, thus displaying inactivity (Figure S18). Consistent with this idea, mutation of the bulky Tyr152 (Y152L, Y152W, and Y152F) is not critical (Figure S19).

These experiments also illustrate that coordination of the substrate to the $(Mg^{2+})_3$ cluster alone is not sufficient for diphosphate abstraction and carbocation formation. If ionization would solely depend on metal binding and mutations of G182 and A183 would just sterically hinder the cyclization cascade, at least the formation of farnesenes should be detected in the respective mutants. Hence, our mutagenesis studies unequivocally demonstrate the importance of the induced-fit mechanism by the newly identified effector triad as the crucial dynamic event in the rearrangement from the open to the closed conformation for efficient catalysis by class I terpene cyclases and progressive substrate turnover (Figure 4).

The presented work elucidates substrate turnover in class I terpene cyclases in unprecedented detail. A novel effector triad located on the G1 helix near its helix-break motif was identified, comprising the strictly conserved PP_i sensor Arg178, the linker Asp181, and the effector Gly182-O. This defined structural architecture, which is also structurally conserved in higher organisms, such as plants and fungi, reveals detailed insights into the initial carbocation formation and regulation. The induced fit ensures that in this class of enzymes product formation only takes place when the active site is firmly locked and not accessible for solvent. Moreover, we propose that the class I terpene cyclase carbocation formation is predominantly triggered by the carbonyl oxygen atom located on the G1/2 helix-break (Gly182-O). The comprehensive understanding of the principles in the catalytic mechanism of class I terpene cyclases might contribute to their future application in advanced semisynthetic chemistry.

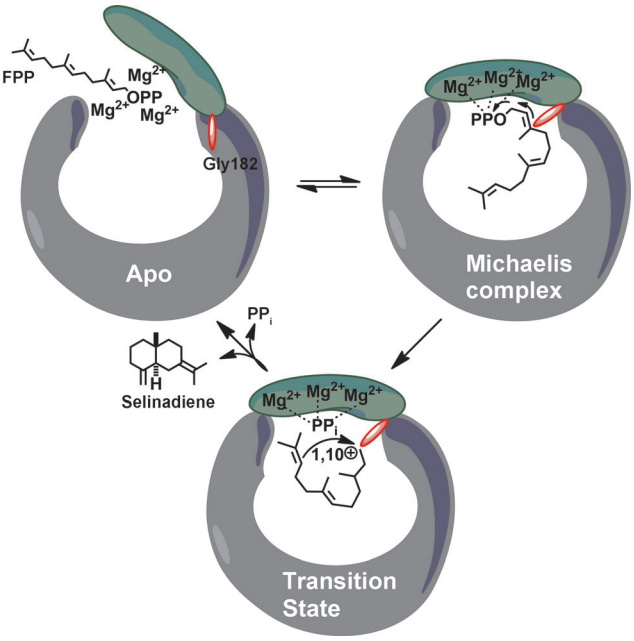

Figure 4. In the apo conformation the active site is accessible for FPP binding and the carbonyl group of Gly182 (red) is orientated outwards the central cavity. Upon substrate binding the PP_i sensor Arg178 forms H-bonds to the $(Mg^{2+})_3$-FPP and to the linker Asp181 (Figure 3 A) with simultaneous closure of the active site. The effector Gly182-O turns inwards, directly pointing towards C3 of FPP, provoking abstraction of PP_i to form the farnesyl cation and to initiate the cyclization cascade (transition state) that starts with a 1,10-cyclization. Once the reaction is completed, the enzyme shifts back to the open conformation (apo) for product release.

Received: March 24, 2014
Published online: May 30, 2014

Keywords: biosynthesis · carbocations · enzyme models · pyrophosphate sensor · terpenoids

 © 2014 Wiley-VCH Verlag GmbH & Co. KGaA, Weinheim

[1] J. S. Dickschat, *Nat. Prod. Rep.* **2011**, *28*, 1917 – 1936.
[2] J. A. Aaron, X. Lin, D. E. Cane, D. W. Christianson, *Biochemistry* **2010**, *49*, 1787 – 1797.
[3] M. J. Rynkiewicz, D. E. Cane, D. W. Christianson, *Proc. Natl. Acad. Sci. USA* **2001**, *98*, 13543 – 13548.
[4] E. Y. Shishova, L. Di Constanzo, D. E. Cane, D. W. Christianson, *Biochemistry* **2007**, *46*, 1941 – 1951.
[5] C. M. Starks, K. Back, J. Chappell, J. P. Noel, *Science* **1997**, *277*, 1815 – 1820.
[6] M. Köksal, Y. Jin, R. M. Coates, R. Croteau, D. W. Christianson, *Nature* **2011**, *469*, 116 – 120.
[7] P. Baer, P. Rabe, C. A. Citron, C. C. de Oliveira Mann, N. Kaufmann, M. Groll, J. S. Dickschat, *ChemBioChem* **2014**, *15*, 213 – 216.
[8] D. Arigoni, *Pure Appl. Chem.* **1975**, *41*, 219 – 245.
[9] D. E. Cane, M. Tandon, P. Prabhakaran, *J. Am. Chem. Soc.* **1993**, *115*, 8103 – 8106.
[10] D. E. Cane, M. Tandon, *J. Am. Chem. Soc.* **1995**, *117*, 5602 – 5603.
[11] D. E. Cane, H. J. Ha, *J. Am. Chem. Soc.* **1986**, *108*, 3097 – 3099.
[12] C. A. Lesburg, G. Zhai, D. E. Cane, D. W. Christianson, *Science* **1997**, *277*, 1820 – 1824.
[13] E. Oldfield, F. Y. Lin, *Angew. Chem.* **2012**, *124*, 1150 – 1163; *Angew. Chem. Int. Ed.* **2012**, *51*, 1124 – 1137.
[14] D. W. Christianson, *Chem. Rev.* **2006**, *106*, 3412 – 3442.
[15] H. A. Gennadios, V. Gonzalez, L. Di Costanzo, A. Li, F. Yu, D. J. Miller, R. K. Allemann, D. W. Christianson, *Biochemistry* **2009**, *48*, 6175 – 6183.
[16] M. Köksal, W. K. Chou, D. E. Cane, D. W. Christianson, *Biochemistry* **2012**, *51*, 3011 – 3020.
[17] P. Rabe, J. S. Dickschat, *Angew. Chem.* **2013**, *125*, 1855 – 1857; *Angew. Chem. Int. Ed.* **2013**, *52*, 1810 – 1812.
[18] J. Kim, S. Matsuyama, T. Suzuki, *J. Labelled Compd. Radiopharm.* **2004**, *47*, 921 – 934.
[19] G. L. Lange, C. Gottardo, *Synth. Commun.* **1990**, *20*, 1473 – 1479.
[20] A. B. Woodside, Z. Huang, C. D. Poulter, *OOrg. Synth. Coll.* **1993**, *8*, 616 – 621.
[21] F. H. Niesen, H. Berglund, M. Vedadi, *Nat. Protoc.* **2007**, *2*, 2212 – 2221.
[22] D. A. Dougherty, *Science* **1996**, *271*, 163 – 168.
[23] J. M. Caruthers, I. Kang, M. J. Rynkiewicz, D. E. Cane, D. W. Christianson, *J. Biol. Chem.* **2000**, *275*, 25533 – 25539.
[24] N. L. Brock, S. R. Ravella, S. Schulz, J. S. Dickschat, *Angew. Chem.* **2013**, *125*, 2154 – 2158; *Angew. Chem. Int. Ed.* **2013**, *52*, 2100 – 2104.
[25] M. Chen, N. Al-lami, M. Janvier, E. L. D′Antonio, J. A. Faraldos, D. E. Cane, R. K. Allemann, D. W. Christianson, *Biochemistry* **2013**, *52*, 5441 – 5453.
[26] D. A. Whittington, M. L. Wise, M. Urbansky, R. M. Coates, R. B. Croteau, D. W. Christianson, *Biochemistry* **2002**, *24*, 15375 – 15380.
[27] D. C. Hyatt, B. Youn, Y. Zhao, B. Santhamma, R. M. Coates, R. B. Croteau, C. Kang, *Proc. Natl. Acad. Sci. USA* **2007**, *104*, 5360 – 5365.

 © 2014 Wiley-VCH Verlag GmbH & Co. KGaA, Weinheim